Structure of Heat-Treated Nylon 6 Fibers. I. Application of the Arrhenius Equation

LUIS ALBERTO DE GODOY ORIANI* and ABIGAIL LISBÃO SIMAL†

Universidade Federal de São Carlos, DEMa, Cx. Postal 676, 13560, S. Carlos, SP, Brazil

SYNOPSIS

The changes in lateral order, crystalline perfection index, crystallinity percentage, long period, and shrinkage denote the structural modification due to thermal effects in the heat-treated nylon 6 fibers. The application of the Arrhenius equation to these parameters resulted in two types of behavior: the parameters long period and shrinkage showed linearity in the temperature range of 100–190°C, while the others presented linearity between 150 and 190°C. The first reflects the direct dependence of crystal growth on shrinkage and the latter shows that the necessary energy to promote significant crystal growth and perfection will be reached only at 150°C. In the range of temperature from 100 to 150°C the observed increase of crystallinity is associated to chain flexibility allowing rearrangement as well as new crystal formation. This phenomenon seems to be related to the discontinuity observed in the Arrhenius plots in the same range of temperature. © 1992 John Wiley & Sons, Inc.

INTRODUCTION

In order to analyze the structural modification in synthetic fibers due to different thermal treatments, several structural parameters are studied and the possibility of a relationship among them is compared. The most commonly studied parameters are the size and perfection of crystals, crystallinity percentage, shrinkage, orientation, and long period.

The Arrhenius equation has been applied by some authors[1,2] in order to study the structural parameter shrinkage percentage due to thermal treatments in poly(ethylene terephthalate) (PET) and nylon 6,6 fibers, respectively. These studies revealed a linearity behavior, when the variation of the shrinkage percentage was plotted against $1/T$ in accordance to the Arrhenius equation. Although this behavior could be an indication of the possibility of application of the Arrhenius equation to other thermally modified structural parameters, this fact has not been explored.

Thus, in the present work we intend to show that the variation in several studied morphological parameters due to heat treatment is characterized by a thermally activated process that can be represented by an equation of the Arrhenius type. Then, we will be able to show through the calculated activated energies and the linearity behavior of the plots which of the studied parameters are positively interrelated and finally reach a better understanding of the structural modifications due to thermal treatments.

In this study the analyzed fibers will be the nylon 6 fibers with two different draw ratios (3.2x and 3.7x). The conditions of the heat treatment are described in the experimental part of this study.

EXPERIMENTAL

Sample Preparation

Nylon 6 fibers from De Millus S/A (Rio de Janeiro, Brazil) of different draw ratios (3.2x and 3.7x) were submitted to heat treatments under slack conditions at 150, 170, and 190°C for 2 and 5 h. An additional 100°C treatment was realized for 1, 5, and 15 h. The heat treatments were made in an evacuated oven

* Present address: Rhodia S.A (Gerência Técnica Fibras), Rua Pedro Rachid, 846, Santana, C.P. 23, 12213—São José dos Campos-SP, Brazil.

† To whom correspondence should be addressed.

Journal of Applied Polymer Science, Vol. 46, 1973–1985 (1992)
 CCC 0021-8995/92/111973-13

under inert atmosphere. The 3.2x was a multifilament fiber and the 3.7x was a monofilament fiber.

Structural Measurements

Density and crystallinity measurements were made using a flotation method (ASTM-D792-79) by a mixture of n-heptane and carbon tetrachloride.

Shrinkage measurements were made by knowing the length of the fibers before and after treatments. From these values the percentage of shrinkage (ΔS) was calculated through the following expression:

$$\Delta S = \frac{S_0 - S_f}{S_0} \times 100$$

where S_0 = initial length of the fiber and S_f = final length of the fiber.

Wide-angle X-ray scattering measurements were used to calculate lateral order (LO) and crystalline perfection index (CPI). These parameters have been defined elsewhere.[3-6] Small-angle X-ray scattering was applied to obtain the long period (LP). In both wide- and small-angle scattering Ni-filtered CuK_α radiation was used. In the small-angle method a pinhole collimation was used with a specimen to film distance of 29 cm. The wide-angle results were obtained from a diffractometric method.

Birefringence was measured by polarized light microscope, utilizing the compensator technique.

RESULTS AND DISCUSSION

Figure 1 shows the effect of increasing annealing temperature on the crystallinity percentage of the fibers. The major changes in crystallinity for the fibers occurred above 100°C, where the 3.2x fiber presented about 2% more crystallinity than the 3.7x fiber. This difference may be related to a more stable structure of the 3.7x fiber with a higher draw ratio. Also, at higher temperatures (above 150°C), it is observed that the crystallinity reaches a maximum value (around 42% for the 3.2x fiber and around 40% for the 3.7x fiber).

Figure 2 shows that the increase of crystallinity is being followed by some crystal growth above 100°C. But, it is at temperatures above 150°C that the long period presents a deep increase.

The same behavior can be observed for the other parameters analyzed (Figs. 3–6). Thus sufficient thermal energy to promote profound structural modifications is reached only at temperatures near

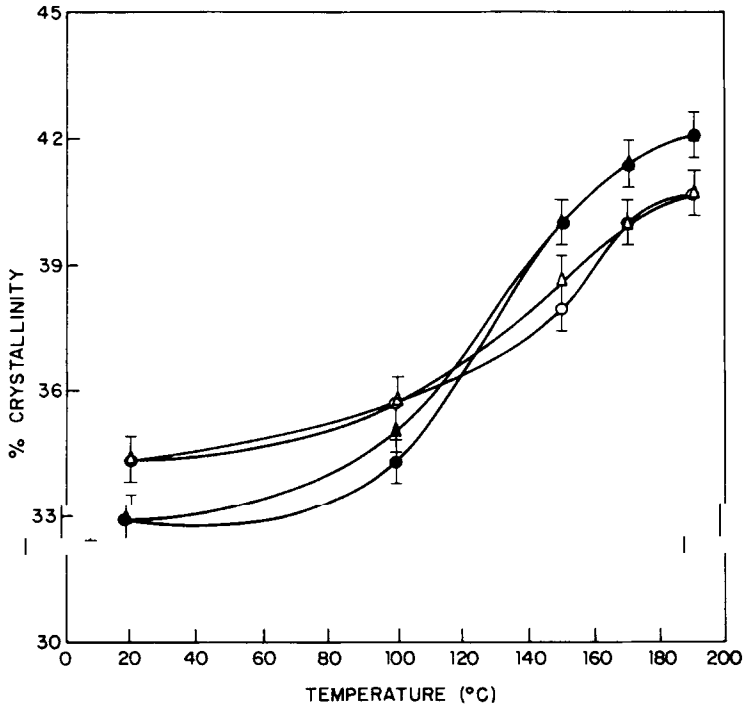

Figure 1 Percent of crystallinity vs. annealing temperatures at different times of treatment for the 3.2x: (▲) 2 h, (●) 5 h and the 3.7x: (△) 2 h, (○) 5 h.

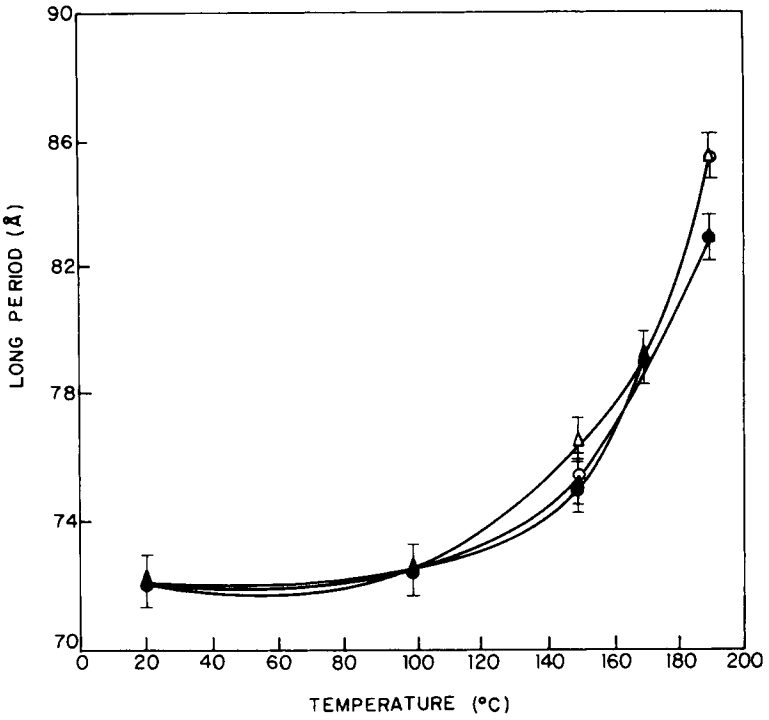

Figure 2 Long period vs. annealing temperatures at different times of treatment for the 3.2x: (▲) 2 h, (●) 5 h, and 3.7x: (△) 2 h, (○) 5 h.

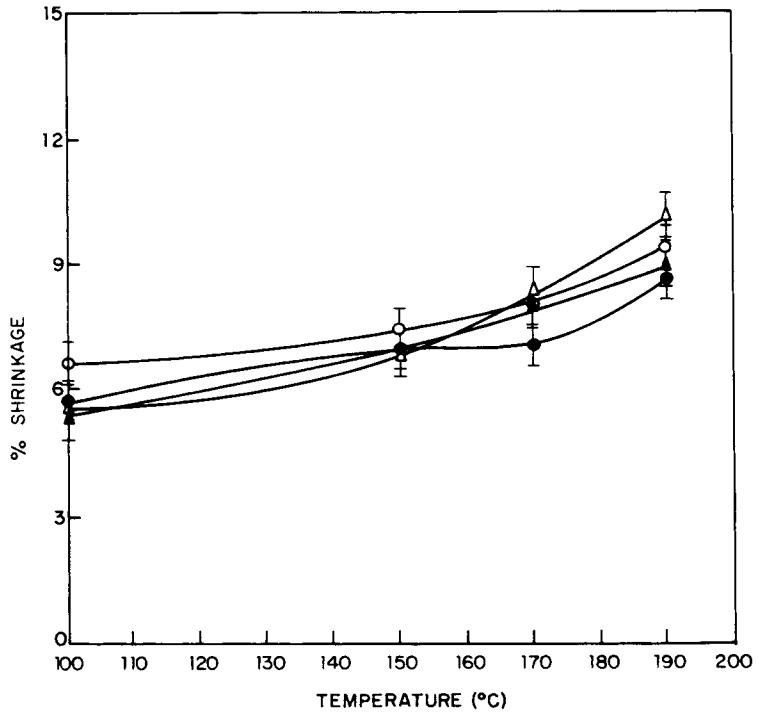

Figure 3 Percent of shrinkage vs. annealing temperatures at different times of treatment for the 3.2x: (▲) 2 h, (●) 5 h and the 3.7x: (△) 2 h, (○) 5 h.

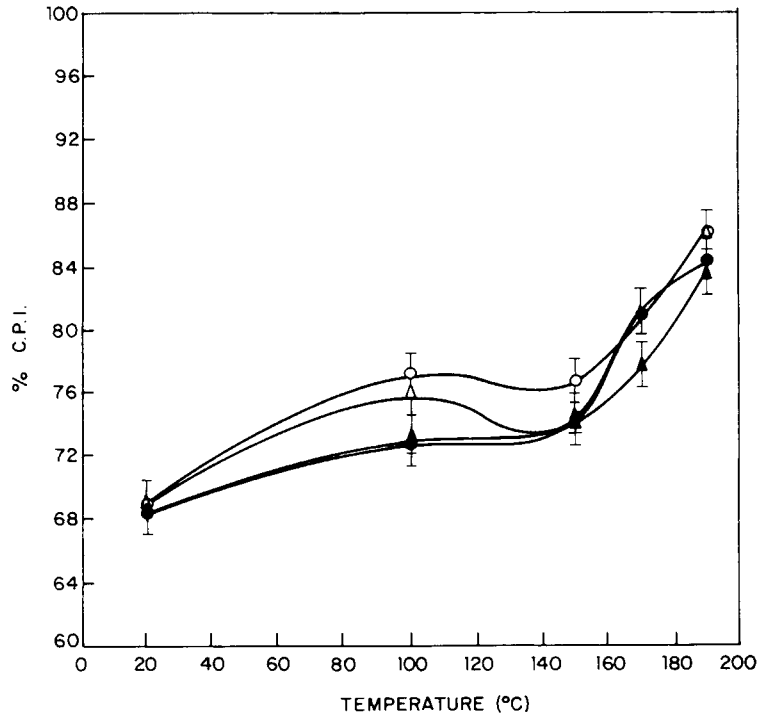

Figure 4 Percent of crystalline perfection index vs. annealing temperatures at different times of treatment for the 3.2x: (▲) 2 h, (●) 5 h and 3.7x: (△) 2 h, (○) 5 h.

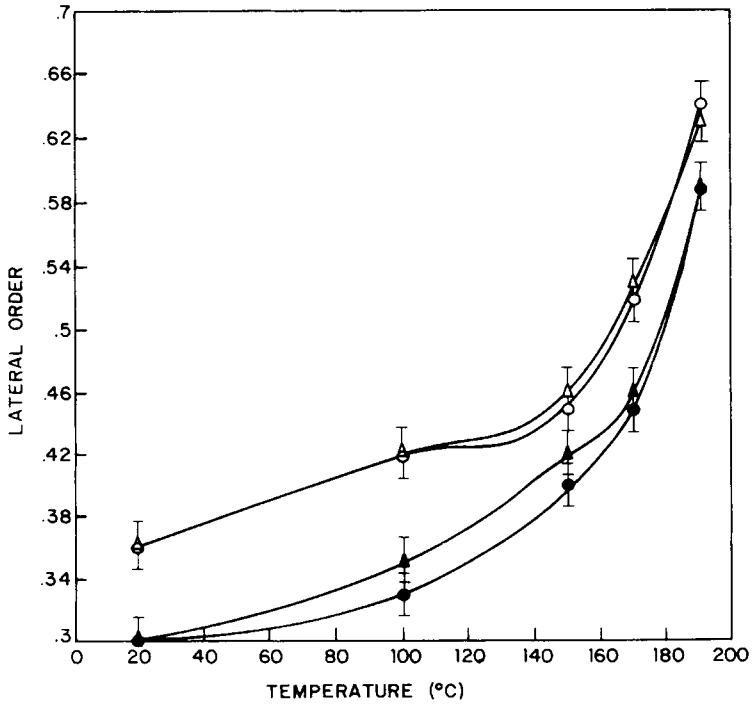

Figure 5 Lateral order vs. annealing temperatures at different times of treatment for the 3.2x: (▲) 2 h, (●) 5 h and 3.7x: (△) 2 h, (○) 5 h.

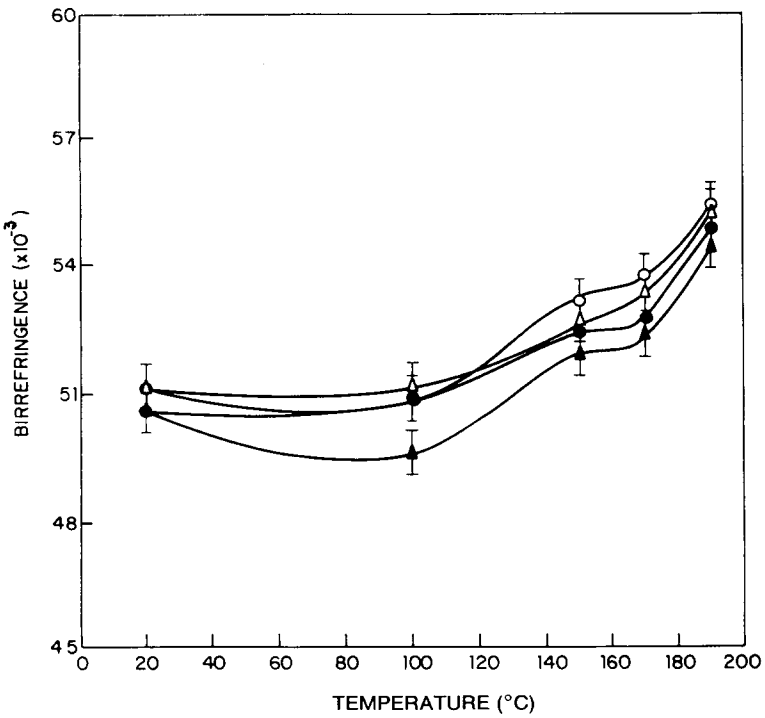

Figure 6 Birefringence vs. annealing temperatures at different times of treatment for the 3.2x: (▲) 2 h, (●) 5 h and 3.7x: (△) 2 h, (○) 5 h.

150°C. Similar results were observed by Park et al.[7] for nylon 6 fibers.

Note that these parameters do not show any tendency to reach an equilibrium in the range of studied temperatures as was observed for the crystallinity parameter. Also, the 3.2x fiber did not show for these parameters results with higher values than the ones obtained for the 3.7x fiber in all analyzed temperatures.

To better understand the thermal effects on the structure of the fibers through the changes on the analyzed parameters, the activation energies relative to the structural transformations were determined using the Arrhenius equation, $\ln K = \Delta E/RT + \text{constant}$, where K is related to the parameter to be studied, T is the absolute temperature, R is the universal gas constant and ΔE, the activation energy. The K values were determined by the following equation:

$$K = \frac{P - P_0}{P_0} \times 100$$

where P is the parameter value at temperature T and P_0 is the parameter value at room temperature (20°C).

The results obtained by the application of the Arrhenius equation to the studied parameters are shown in the Figures 7–11.

The figures show two kinds of behavior: The parameters long period and shrinkage obey the Arrhenius equation, i.e., the linearity exists, in the temperature range of 100–190°C, while the parameters crystallinity, LO, and CPI present linearity between 150 and 190°C only. The calculated activation energies are shown in Table I. The calculations were made in the linearity region.

Thus, it is possible to expect some kind of relationship between shrinkage and long period. This relationship is confirmed by Figure 12, where long period is plotted against shrinkage, and a linearity between these quantities is observed for both fibers. Samuels[8] has shown a similar result for PET fibers, where he suggests the existence of a relationship between the molecular relaxation of noncrystalline regions and the crystallization of his samples.

When crystallinity is plotted against shrinkage (Fig. 13), it appears that as the shrinkage is increasing at higher temperatures, the crystallinity is reaching its maximum. This suggests that shrinkage is a complex process, where the recrystallization occurs accompanied by growth and perfection of the

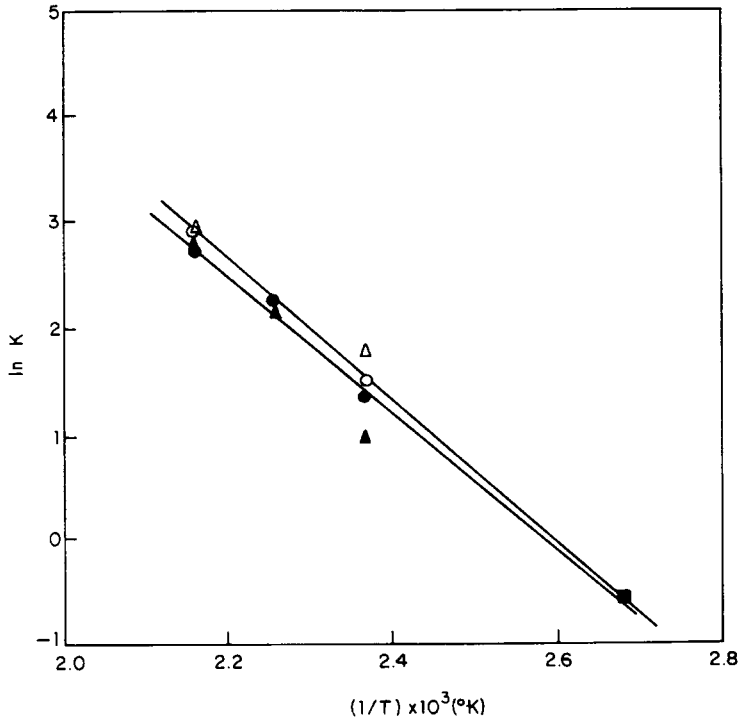

Figure 7 Arrhenius plot for the long period 3.2x: (■, ▲, ●) 1, 2, and 5 h and 3.7x: (□, △, ○) 1, 2, and 5 h.

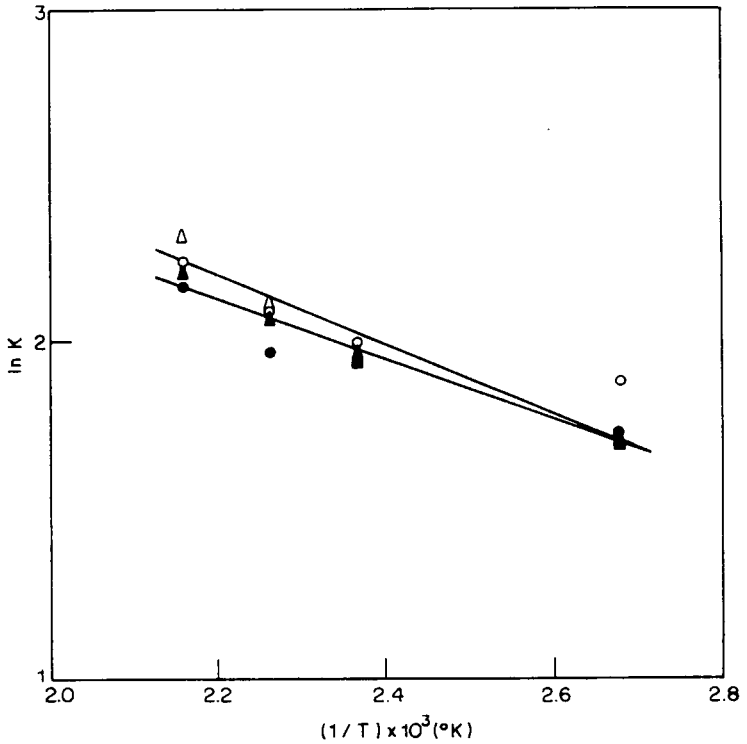

Figure 8 Arrhenius plot for the shrinkage: 3.2x: (■, ▲, ●) 1, 2, and 5 h and 3.7x: (□, △, ○) 1, 2, and 5 h.

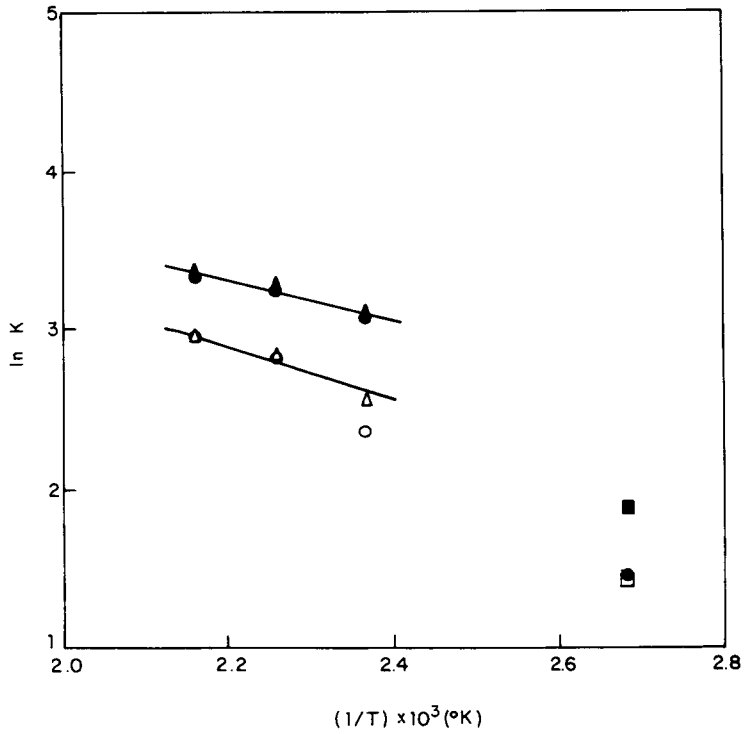

Figure 9 Arrhenius plot for the crystallinity: 3.2x: (■, ▲, ●) 1, 2, and 5 h and 3.7x: (□, △, ○) 1, 2, and 5 h.

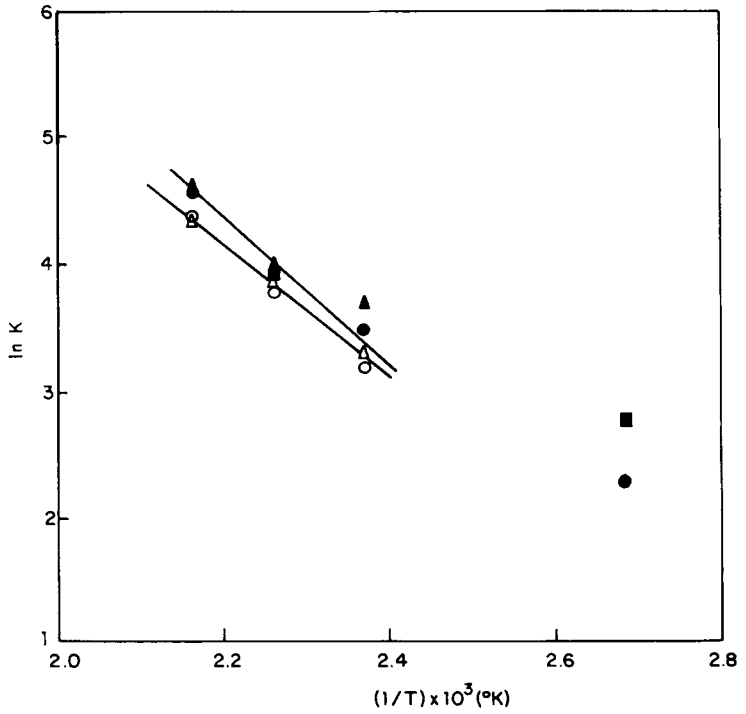

Figure 10 Arrhenius plot for the lateral order: 3.2x: (■, ▲, ●) 1, 2, and 5 h and 3.7x: (□, △, ○) 1, 2, and 5 h.

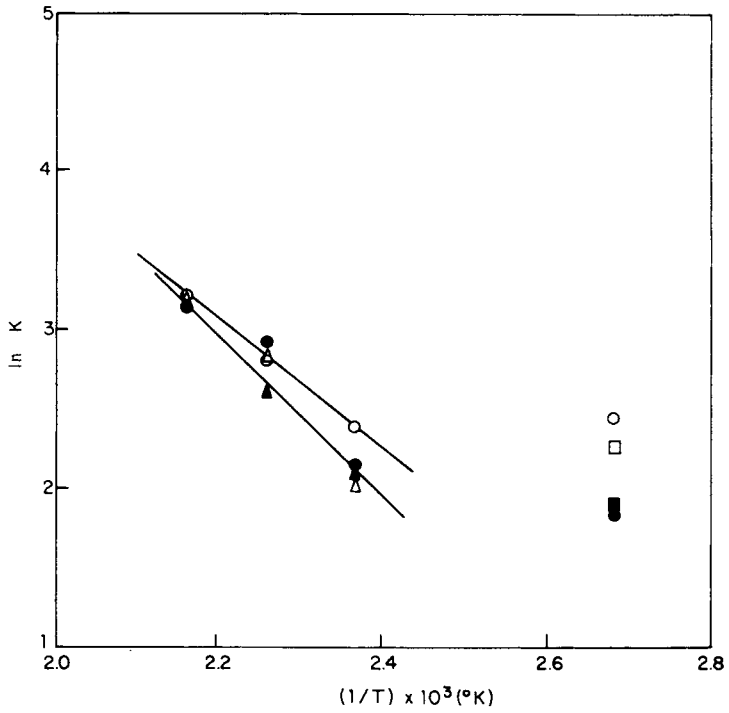

Figure 11 Arrhenius plot for the crystalline perfection index: 3.2x: (■, ▲, ●) 1, 2, and 5 h and 3.7x: (□, △, ○) 1, 2, and 5 h.

crystals. The size of the annealed crystals is a direct function of the relaxation of the noncrystalline regions of the fibers, as confirmed by the linear dependence between long period and shrinkage.

Figures 14–16 confirm once more these results. In these figures, crystallinity is plotted against CPI, LO, and long period. In all cases it is above 150°C, where crystallinity has almost reached its maximum, that the parameters CPI, LO, and long period increase rapidly. Thus, the major transformations related to growth and perfection of the crystals are occurring in this region.

Also, Figures 14–16 show a plateaulike region in the range of temperatures between 100 and 150°C. It seems that the transformations occurring in this region are related to the observed discontinuity in the Arrhenius plots for the same studied parameters. The necessary energy to promote significant crystal growth and perfection will be reached only at 150°C, and these morphological phenomena are associated to shrinkage. In this plateau region only an increase of crystallinity percentage is observed. The little increase of crystal perfection from room temperature to 100°C must be related to elimination of imperfections of the originally presented crystals in the fibers due to processing (spinning and drawing). The increase of crystallinity in this region is very small.

The increase of crystallinity in the plateau region must be associated to an increase of chain flexibility, since in this range of temperature we are working above the T_g of fibers (around 90°C for both fibers). The chain flexibility will allow crystals rearrangement as well as new crystal formation. At higher temperatures (above 150°C) the chain flexibility is very intense allowing what we can call as a second step of the process, i.e., an accentuated growth and perfection of the crystals.

The calculated activation energies from the plots of $\ln K \times 1/T$ (Table I) confirm the earlier conclu-

Table I Activation Energies (ΔE) Calculated from the Tangent of the Straight Lines Observed in Arrhenius Plots

		ΔE (cal/mol)	
Parameters	Range of Temperature	3.2x	3.7x
Crystallinity	150–190	2,592	4,826
Shrinkage	100–190	1,716	1,692
CPI	150–190	9,862	9,828
LO	150–190	9,694	10,630
Long period	100–190	12,900	13,504

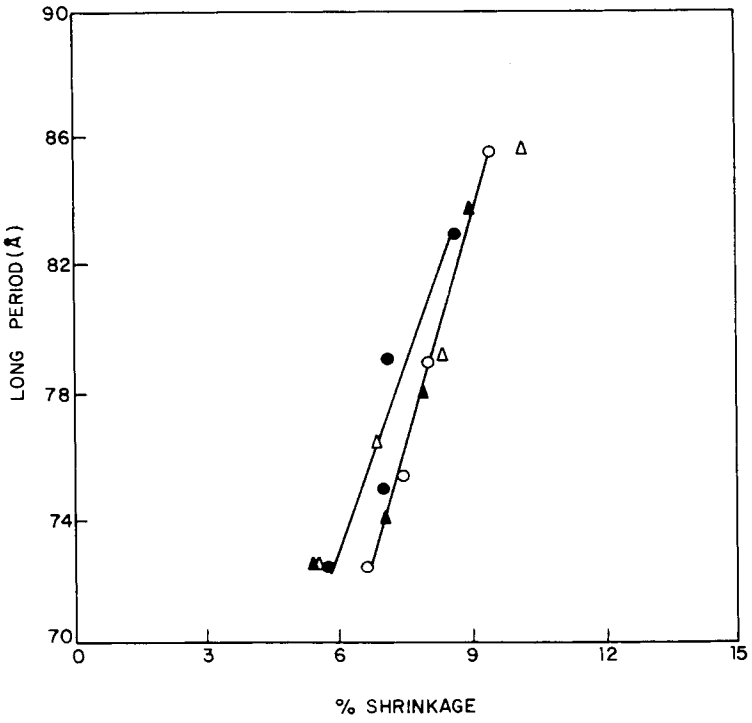

Figure 12 Long period vs. percent of shrinkage at different annealing temperatures and times for the 3.2x: (▲) 2 h, (●) 5 h and the 3.7x: (△) 2 h, (○) 5 h.

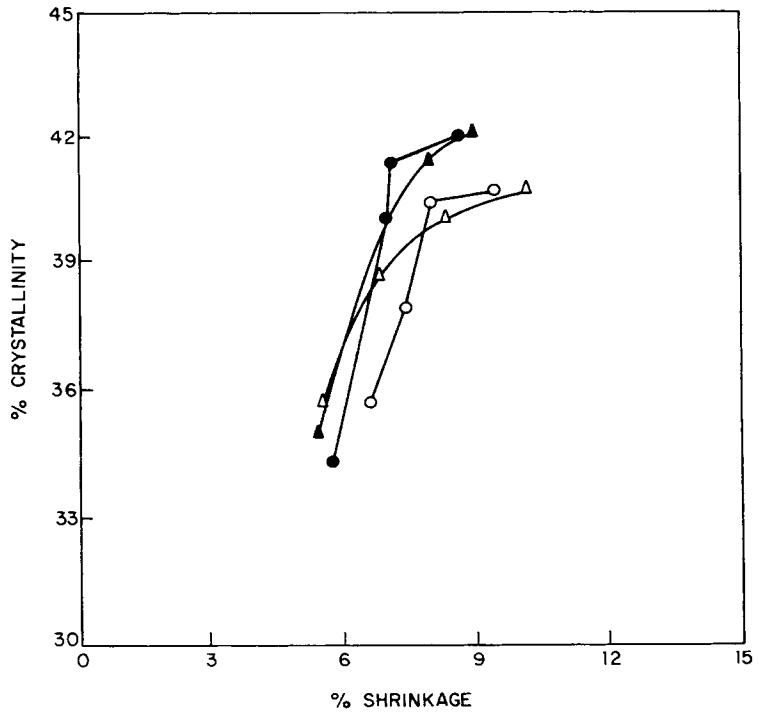

Figure 13 Percent of crystallinity vs. percent of shrinkage at different annealing temperatures and times for the 3.2x: (▲) 2 h, (●) 5 h and 3.7x: (△) 2 h, (○) 5 h.

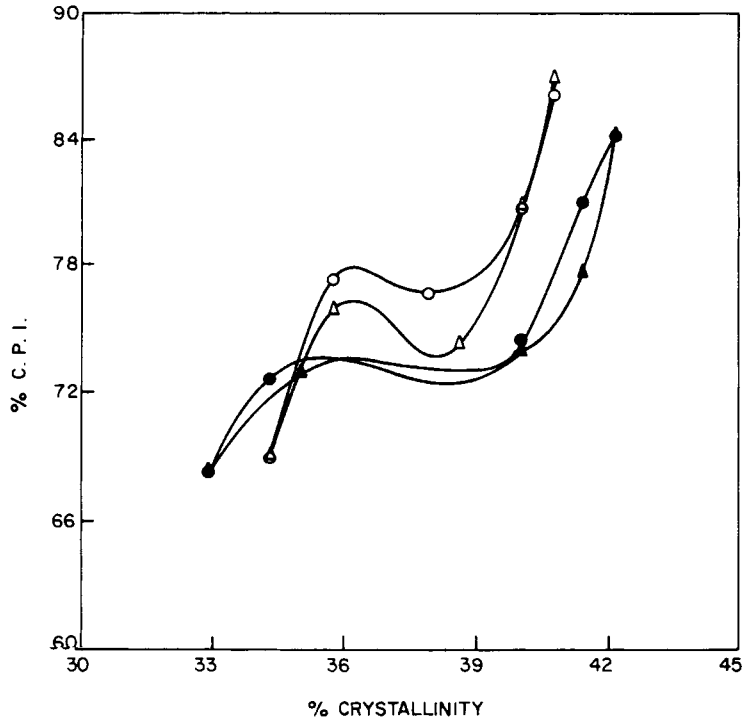

Figure 14 Percent of crystalline perfection index vs. percent of crystallinity at different annealing temperatures and times for the 3.2x: (▲) 2 h, (●) 5 h and 3.7x: (△) 2 h, (○) 5 h.

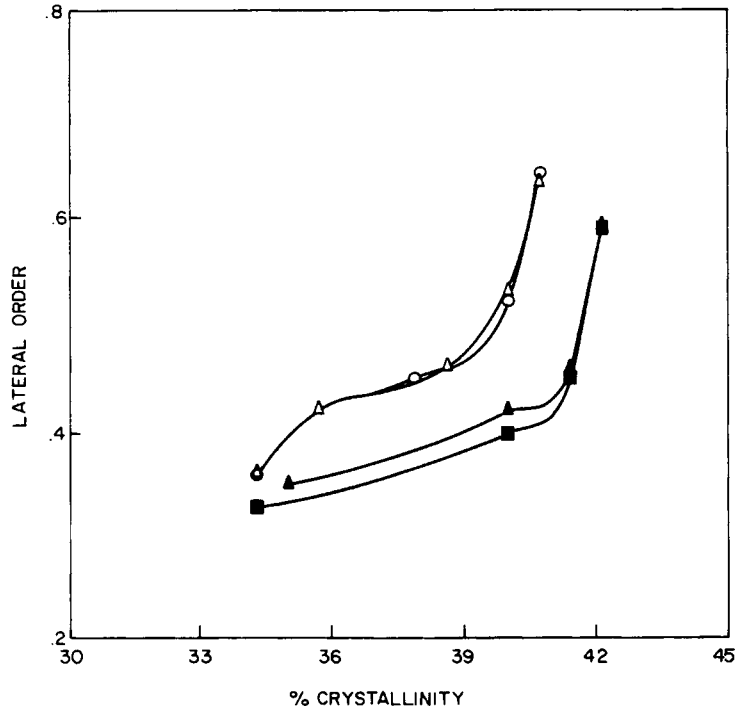

Figure 15 Lateral order vs. percent of crystallinity at different annealing temperatures and times for 3.2x: (▲) 2 h, (●) 5 h and 3.7x: (△) 2 h, (○) 5 h.

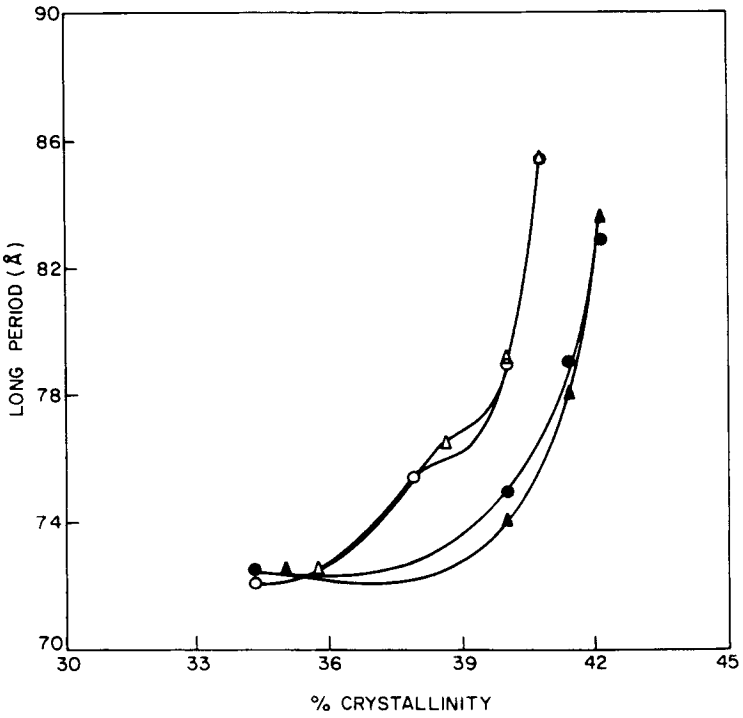

Figure 16 Long period vs. percent of crystallinity at different annealing temperatures and times for the 3.2x: (▲) 2 h, (●) 5 h and the 3.7x: (△) 2 h, (○) 5 h.

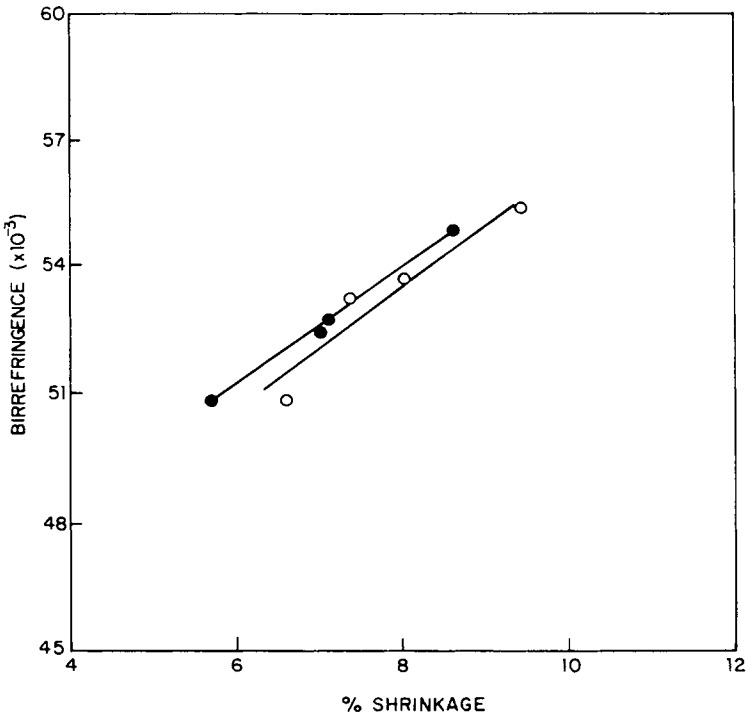

Figure 17 Birefringence vs. percent of shrinkage at different annealing temperatures (5 h) for the (●) 3.2x and (○) 3.7x fibers.

sion of a more stable structure for the 3.7x fiber. This fiber needs a much higher activation energy (of about 86% higher) than the 3.2x fiber to have an increase of crystallinity in the same range of temperatures. The calculated activation energies for the remainder of parameters did not show significant differences between the fibers, suggesting that these transformations require the same level of energy.

A comparison among the parameters reveals that shrinkage presents the lowest value of activation energy. This result demonstrates the ease of these fibers to relieve internal residual tensions due to processing and the true dependence of shrinkage on the noncrystalline regions. Parameters such as CPI, LO, and long period are more related to modifications within the crystals where strong intermolecular interactions prevail.

Another interesting observation relative to these figures is the time independence of the analyzed parameters after 1 h of treatment in the studied range of temperatures. The same observation was shown by Parker and Lindenmeyer,[9] where their nylon 6 fibers did not show any significant structural changes after 2 h of heat treatments at temperatures of 50–210°C.

The effects of the shrinkage on the birefringence of the fibers are also of interest and are shown in the Figure 17.

In general, it is expected that the shrinkage of an oriented fiber due to relaxation of noncrystalline regions would promote a decrease in the birefringence, since disorientation of crystals might be happening. But for these nylon 6 fibers, as Figure 17 shows, an increase of the birefringence with shrinkage is observed.

The observed results are an indication that the recrystallization due to temperature effects is occurring in a preferential direction or parallel to the fiber axis. Similar results have been described by other authors[10,11] for different materials including nylon 6.

The X-ray patterns for the small-angle diffraction (Fig. 18) are in good agreement with these conclusions. The control fibers (nontreated) show an arc

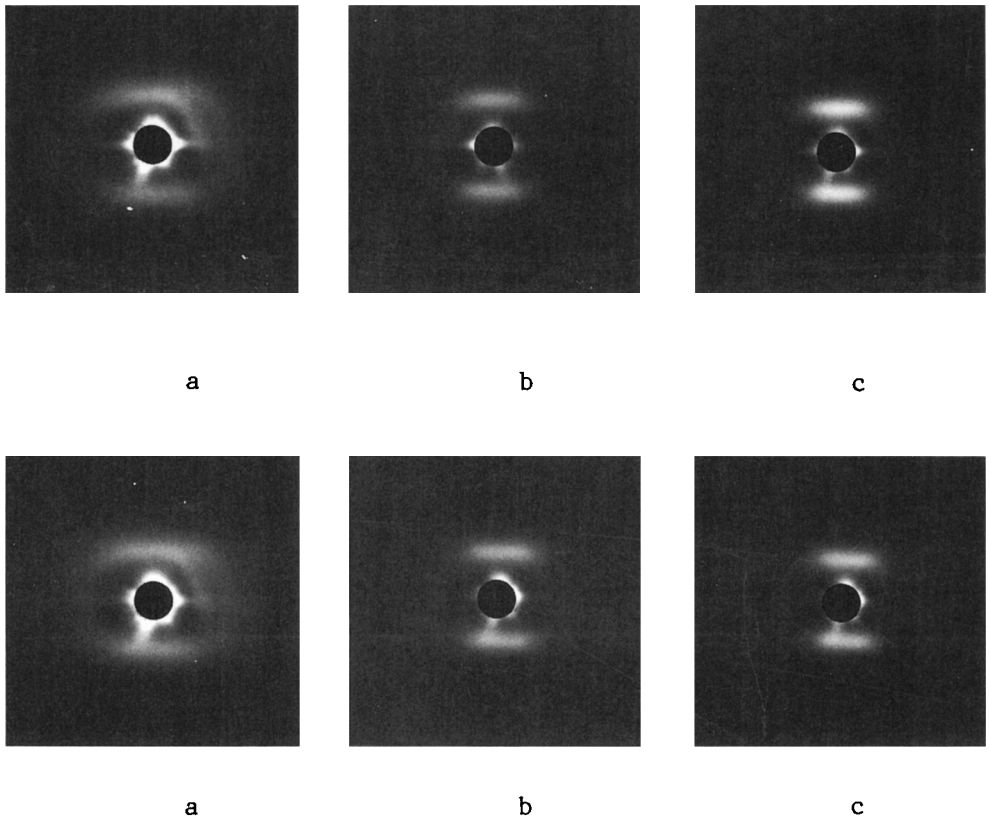

Figure 18 SAXS for the 3.2x (upper photophaps) and 3.7x fibers: (a) control, (b) 170°C, (c) 190°C.

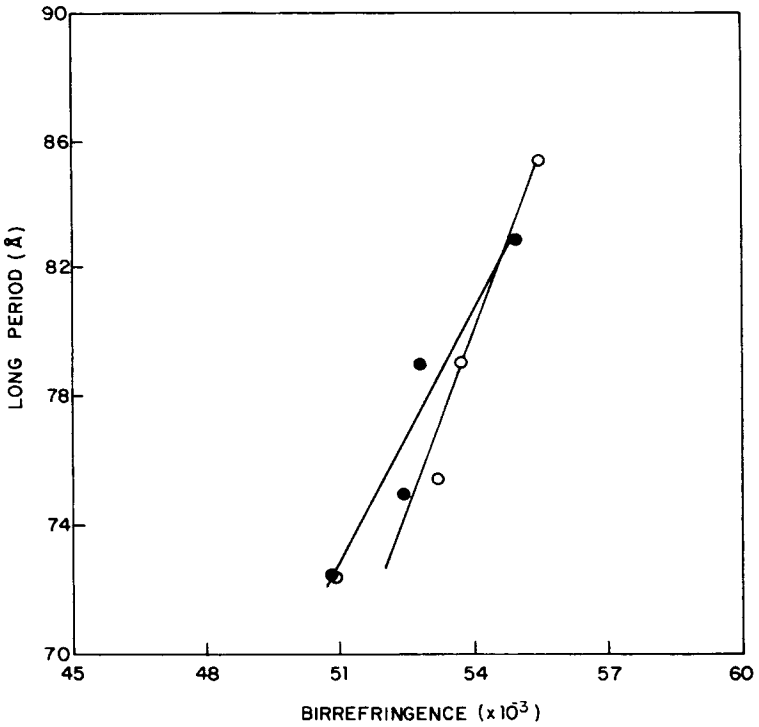

Figure 19 Long period vs. birefringence at different annealing temperatures (5 h) for the (●) 3.2x and (○) 3.7x fibers.

similar to small-angle patterns, while the treated ones present horizontal streaks. Horizontal streaks in small-angle patterns denote in general a preferential crystalline orientation to the fiber axis. When the orientation decreases, the small-angle patterns become arclike. A totally random crystalline orientation would present a circular diffraction pattern.[12]

The linear tendency observed in Figure 17 is also observed in Figure 19, where the birefringence was plotted as a function of the long period for both fibers. This behavior seems to be in agreement with the earlier results, where long period showed to be linearly dependent of the shrinkage (see Fig. 12). Crystal growth due to shrinkage is occurring with a preferential orientation, i.e., the direction of the fiber axis.

This research was supported in part by FINEP and in part by FAPESP, Brazil. We would like to express our appreciation to Y. Mascarenhas and to A. Trombella for their permission and help with the utilization of the X-ray equipments of the Physics Department, USP-São Carlos, Brazil, and to D. B. Gimenez and to C. E. Carniato for the photographs and drawings, respectively.

REFERENCES

1. W. O. Statton, in *The Setting of Fibres and Fabrics*, J. W. S. Hearle and L. W. C. Miles, eds., Merrow, London, 1971.
2. V. B. Gupta and S. Kumar, *J. Appl. Polym. Sci.*, **26,** 1865 (1981).
3. A. Manjunath, A. Venkataraman, and T. Stephen, *J. Appl. Polym. Sci.*, **17,** 1091 (1973).
4. P. F. Dismore and W. O. Statton, *J. Polym. Sci. Part C*, **13,** 133 (1966).
5. H. M. Heuvel, R. Hiusman, and J. C. K. Lind, *J. Polym. Sci. Phys. Ed.*, **14,** 921 (1976).
6. R. A. Moore and H. D. Weigmann, *Text. Res. J.*, **56,** 180 (1986).
7. J. B. Park, K. L. Devries, and W. O. Statton, *J. Macrom. Sci., B,* **15**(2), 229 (1978).
8. R. J. Samuels, *J. Polym. Sci. Part A2,* **10,** 781 (1972).
9. J. P. Parker and D. H. Lindenmeyer, *J. Appl. Polym. Sci.*, **21,** 821 (1977).
10. A. Ziabicki, *Fundamentals of Fibre Formation,* London, Wiley-Interscience, 1976.
11. D. R. Subrhmanian and A. Venkataraman, *J. Macrom. Sci., B,* **18**(2), 177 (1980).
12. A. Peterlin, *Text. Res. J.*, **42,** 20 (1972).

Received March 16, 1990
Accepted February 21, 1992